



De Almeida, G., Bates, P., & Ozdemir, H. (2016). Modeling urban floods at submeter resolution: challenges or opportunities for flood risk management? *Journal of Flood Risk Management*.
<https://doi.org/10.1111/jfr3.12276>

Peer reviewed version

Link to published version (if available):
[10.1111/jfr3.12276](https://doi.org/10.1111/jfr3.12276)

[Link to publication record in Explore Bristol Research](#)
PDF-document

This is the author accepted manuscript (AAM). The final published version (version of record) is available online via Wiley at <http://onlinelibrary.wiley.com/doi/10.1111/jfr3.12276/full> . Please refer to any applicable terms of use of the publisher.

University of Bristol - Explore Bristol Research

General rights

This document is made available in accordance with publisher policies. Please cite only the published version using the reference above. Full terms of use are available:
<http://www.bristol.ac.uk/red/research-policy/pure/user-guides/ebr-terms/>

Modeling urban floods at sub-meter resolution: challenges or opportunities for flood risk management?

Gustavo A. M. de Almeida^{a,*}, Paul Bates^b, Hasan Ozdemir^c,

^a*University of Southampton, Faculty of Engineering and the Environment, SO171BJ, UK.*

^b*University of Bristol, School of Geographical Sciences, University Rd., Bristol BS8 1SS, UK.*

^c*Geography Department, Istanbul University, 34459 Instabul, Turkey.*

Abstract

In this article we investigate the influence of fine scale changes in the elevation of urban terrains on the dynamics and final distribution of flood inundation generated by intense rainfall. Numerical experiments have been performed combining 2D shallow-water model with extremely fine resolution (10 cm) terrain data. Our results reveal that localized, decimetric-scale alterations in the elevation of streets can lead to remarkable differences in the flood inundation. These results confirm the important role played by finely resolved and accurate terrain data in capturing flow patterns that have a central impact on model predictions of flood inundation. More importantly, we argue that the sensitivity of flood inundation to small-scale topographical features paves the way to new opportunities for flood risk management measures. In particular, engineering flood resilient urban surfaces (FRUS) using fine resolution models has a potential to considerably reduce flood impacts at a relatively low cost.

Keywords: urban flood, modelling, terrestrial LiDAR

1. Introduction

It is an unfortunate and often tragic combination of factors that places urban flooding amongst the most damaging and costly of all natural hazards. Worldwide, a relatively frequent occurrence of heavy rainfall storms combine with high levels of human exposure and high-value and vulnerable assets to produce multi-billion losses every year. In a world of rapid urbanization and

*
Preprint submitted to *Environmental Modelling & Software* August 14, 2015
Email address: g.dealmeida@soton.ac.uk (Gustavo A. M. de Almeida)

31 considering the prospect of strongly adverse climate change effects, under-
32 standing and mitigating urban flood risks is eliciting widespread concern and
33 has become an issue of the highest priority.

34 Among different sources of flooding that can occur in urban areas (e.g.
35 river, coastal, groundwater), surface water flooding (i.e. flood resulting from
36 intense excess rainfall) is often responsible for a significant proportion of
37 flood losses. For instance, the Environment Agency of England and Wales
38 estimates that 3.8 million properties are at risk of surface flooding (*EA*, 2009)
39 in England and Wales. A drastic example of this exposure occurred during
40 the summer of 2007, when two thirds of the 55,000 inundation of properties
41 have been attributed to surface water (*DEFRA*, 2008; *Evans et al*, 2008).
42 In spite of the relevance to current and future generations, a comprehensive
43 understanding of the dynamics of surface water urban inundation, as well
44 as the development of methods to accurately model and mitigate its conse-
45 quences are still in their infancy when compared to the substantial progress
46 achieved over decades of research in river and coastal flooding. While models
47 of sewerage systems date back to the early 70's (*Delleur*, 2003), the devel-
48 opment and application of the first coupled sewer-surface flow models only
49 emerged during the first decade of the 21st century (*Djordjevic et al*, 1999).
50 In addition, prevention and mitigation of urban flooding has historically been
51 limited in scope, and almost exclusively linked to the appropriate design and
52 sizing of the sewerage system, a vision that has only recently been broad-
53 ened to include the concepts of Sustainable Drainage Systems (SuDS). Little
54 attention has been given to a thorough understanding of the role played by
55 urban topography (in particular sub-meter scale) on the behavior of floods.
56 This is despite the fact that under medium to extreme rainfall events (when
57 the sewer system is usually surcharged) most of the flood water is expected
58 to be carried as overland flow (e.g. *Mark et al*, 2004; *Mignot et al*, 2006), in
59 which case the layout of surface pathways will largely dictate what areas of
60 the urban terrain will be inundated.

61 Even though during intense rainfall events large parts of urban areas may
62 be exposed to relatively high flow depths, this usually occurs as a result of the
63 accumulation (in terrain depressions or lowland areas) of water previously
64 routed from the urban catchment along roads and other flow paths. The
65 transport of surface flow along these pathways is a phenomenon of shallow
66 water (i.e. typically $< 20\text{cm}$ deep) that can move at relatively high velocities.
67 This type of flow is controlled by small-scale features of the urban terrain such
68 as the height of curbs, the shape and dimensions of road cambers, as well as by

the connectivity of roads and pathways. The road network can be particularly efficient in transporting water across the urban domain and therefore plays an important role in the ultimate distribution of flooded areas. Capturing the effects of these elements in a two dimensional (2D) model requires very fine resolution topography (i.e. sub-meter resolution, as discussed in *Ozdemir et al*, 2013), which translates into extremely high computational times that are often unfeasible in most practical applications. This results from the fact that the computational time of explicit two-dimensional models usually used for flood simulations scales with the resolution of the mesh raised to the power of three. For instance, refining a mesh from 1 m to 10 cm translates into a $1000\times$ increase in the simulation time.

As a response to the above computational barrier, a number of practical modeling abstractions and simplifications have emerged, which attempt to overcome this limitation and to achieve simulation run times that are compatible with available computational resources. Particular efforts have been devoted to models that conceptualize the surface component of urban floods as a set of elements such as small catchments and/or ponds that are interconnected by 1D channels that represent the road network (e.g. *Mark et al*, 2004; *Nasello and Tucciarelli*, 2005; *Maksimovic et al*, 2009; *Leandro et al.*, 2009), in a similar way to the first river network models of the late 1970's (e.g. *Cunge*, 1980). The coupling of this representation of the surface flow with a sewerage network model is often described as a 1D-1D model, as opposed to the 2D-1D approach, in which a two dimensional model is used to simulate the overland component of the flow. Some of the limitations of the 1D representation of surface flow (such as the dependency on user-defined schemes, such as 1D network of pathways and storage elements) have been previously exposed (*Mark et al*, 2004; *Leandro et al.*, 2009), while other aspects related to the upscaling of sub-meter features remain largely unknown.

Two-dimensional models used in urban flooding are usually based on the shallow water equations (*Mignot et al*, 2006; *Bazin et al*, 2014), and simplified forms of these equations such as the zero inertial (e.g. *Nasello and Tucciarelli*, 2005; *Leandro et al.*, 2009) and local inertial approximations (e.g. *Aronica and Lanza*, 2005; *Fang and Su*, 2005; *Bates et al*, 2010; *de Almeida et al*, 2012; *de Almeida and Bates*, 2013), or even simpler formulations (*Sampson et al*, 2012), have also been widely adopted to speed up simulations. Another strategy to reduce the computational burden of 2D models focuses on defining sub-grid abstractions that resolve some of the complexities of the urban relief, which is modeled at coarse resolution (e.g. $10 \sim 100m$).

107 Among this type of models, those adopting the concept of porosity to de-
 108 scribe urban features such as buildings have attracted significant attention
 109 (e.g. *Molinaro et al*, 1994; *Sanders et al*, 2008; *Soares-Frazao et al*, 2008;
 110 *Guinot*, 2012 to cite but a few). While this approach correctly represents
 111 some of the physics operating at intermediate resolution scales (such as the
 112 influence of buildings on mass and momentum conservation, which is gov-
 113 erned by building dimensions and spacings) and perform well in representing
 114 catastrophic flood events (e.g. dam-break induced), it lacks the ability to
 115 capture wetting and drying, blockage and other directional effects that are
 116 governed by considerably fine scale topographical features.

117 To date, two dimensional modeling of urban floods has been performed
 118 almost exclusively using digital elevation models (DEMs) with resolutions of
 119 1 m or coarser (e.g. *Mark et al*, 2004; *Fang and Su*, 2005; *Aronica and Lanza*,
 120 2005; *Gallegos et al*, 2009; *Leandro et al.*, 2009; *Maksimovic et al*, 2009; *Gal-*
 121 *lien et al*, 2011; *de Almeida et al*, 2012). Advances in computational resources
 122 and methods combined with the recent availability of sub-meter resolution
 123 terrestrial LiDAR data have enabled the first two-dimensional simulations of
 124 urban inundation to be performed at resolutions as low as 10 cm (*Ozdemir*
 125 *et al*, 2013). These extremely fine resolution simulations have shown that
 126 differences in model predictions persist even as the mesh resolution is re-
 127 fined from 50 cm to 10 cm. Implicit to this dependency of simulation results
 128 on mesh resolution are two different albeit interrelated issues. Firstly, the
 129 shape of different terrain features are degraded as the resolution is coars-
 130 ened, which particularly affects the flow conveyance of road cambers and the
 131 storage capacity of different elements (e.g. depression storage). Secondly,
 132 and arguably more importantly for shallow water flows, is the fact that the
 133 elevation of local peaks are closely approximated at fine resolution, but are
 134 in general underestimated at coarser resolution as a result of the increased
 135 average distance from the peaks to sampled points. For example, considering
 136 a road camber with average cross slope of 4%, the maximum error introduced
 137 to the vertical position of the crown by a 5 m resolution sampling is 10 cm.
 138 This is of the same order of magnitude as typical flood depths that are ob-
 139 served at road networks, and is expected to allow the model to incorrectly
 140 route water along directions that would be topographically blocked in reality.

141 If the sensitivity of flood inundation to decimetric-scale elevation changes
 142 confirmed, it has two important impacts on the future of flood risk assess-
 143 ment and management. Firstly, it highlights the need for finely resolved and
 144 accurate topography, which poses significant challenges to current genera-

145 tion computational resources. Secondly, it paves the way for a range of new
 146 opportunities for urban drainage methods that have not been previously ex-
 147 plored, and which have the potential to considerably reduce the impacts of
 148 extreme storms at relatively low cost.

149 The value of finely resolved topography in flood inundation modeling is
 150 an issue of intense recent debate, particularly when analyzed in the broader
 151 context of other sources of uncertainties that are inherently present in prac-
 152 tical flood risk assessments (e.g. *Dottori et al*, 2013 and references therein).
 153 While results from grid refinement sensitivity analysis (e.g. *Ozdemir et al*,
 154 2013) indicate that horizontal resolution plays an important role on model
 155 results, it is unclear the extent to which small perturbations in the elevation
 156 can produce significant changes to the patterns of surface flood inundation.
 157 In this article an extremely fine resolution (10 cm) description of the urban
 158 terrain is combined with a highly accurate and robust finite volume shallow
 159 water model to analyze the effects of decimetric scale and localised changes
 160 in the topography on the dynamics and outcomes of urban flooding. This
 161 relation is explored by introducing small modifications in the elevation of
 162 the original 10 cm resolution DEM, and comparing the simulation results
 163 against those obtained with the undisturbed DEM. Even though direct mod-
 164 elling of floods at such fine resolution (i.e. 10 cm) is unfeasible for any
 165 practical purposes in the foreseeable future, they offer a unique opportunity
 166 to clarify the extent to which decimetric scale terrain features control flood
 167 dynamics. The results of this analysis are then used to open a discussion
 168 on the challenges and opportunities that are intrinsically associated with the
 169 topography-impact nexus.

170 2. Numerical model

171 The model used here is based on the two-dimensional shallow water equa-
 172 tions

$$\frac{\partial \mathbf{U}}{\partial t} + \frac{\partial \mathbf{F}(\mathbf{U})}{\partial x} + \frac{\partial \mathbf{G}(\mathbf{U})}{\partial y} = \mathbf{S}_1(x, y, \mathbf{U}) - \mathbf{S}_2(x, y, \mathbf{U}) \quad (1)$$

173 where the $\mathbf{U}(x, y, t)$ is the vector of conserved variables, $\mathbf{F}(\mathbf{U})$ and $\mathbf{G}(\mathbf{U})$ are
 174 the flux vectors in the x and y directions, respectively, and $\mathbf{S}_1(x, y, \mathbf{U})$ and

175 $\mathbf{S}_2(x, y, \mathbf{U})$ are the slope and friction source terms, respectively:

$$\mathbf{U} = \begin{bmatrix} h \\ hu \\ hv \end{bmatrix}, \mathbf{F} = \begin{bmatrix} hu \\ hu^2 + \frac{1}{2}gh^2 \\ huv \end{bmatrix}, \mathbf{G} = \begin{bmatrix} hv \\ huv \\ hv^2 + \frac{1}{2}gh^2 \end{bmatrix},$$

$$\mathbf{S}_1 = \begin{bmatrix} 0 \\ ghS_{ox} \\ ghS_{oy} \end{bmatrix}, \mathbf{S}_2 = \begin{bmatrix} 0 \\ ghS_{fx} \\ ghS_{fy} \end{bmatrix},$$

176 h is the water depth, u and v are the x and y components of the velocity, g
 177 is the acceleration due to gravity, S_{ox} and S_{oy} are the x and y components
 178 of the bed slope (i.e. $-\partial z/\partial x$ and $-\partial z/\partial y$, respectively, where z is the
 179 bed elevation) and S_{fx} and S_{fy} the corresponding components of the friction
 180 slope. The numerical model solves the integral form of eqs. (1):

$$\frac{\partial}{\partial t} \int_{\Omega} \mathbf{U} d\Omega + \oint_{\partial\Omega} (\mathbf{E} \cdot \mathbf{n}) dl = \int_{\Omega} (\mathbf{S}_1 - \mathbf{S}_2) d\Omega \quad (2)$$

181 where \mathbf{E} is the 3×2 flux tensor $\mathbf{E} = (\mathbf{F}, \mathbf{G})$, Ω and $\partial\Omega$ respectively denote an
 182 arbitrary domain and its boundary, and \mathbf{n} is a unit outward vector normal
 183 to $\partial\Omega$. Eqs. 2 can be obtained by integrating (1) over Ω and then applying
 184 Gauss's theorem to the integral of the flux terms.

The computational domain is discretised using an unstructured mesh composed of triangular cells (Figure 1). Eqs. 2 are integrated numerically using a first order Godunov finite volume scheme, and a fractional step (e.g. described in *LeVeque*, 2002). First the cell-averaged value of the conserved variables \mathbf{U}_i in cell Ω_i are updated considering the flux terms (homogeneous part) and the bed slope, but neglecting the friction source term. \mathbf{S}_1 is evaluated with the method of *Valiani and Begnudelli* (2006), by which the area integral of \mathbf{S}_1 in (2) is transformed into a boundary integral that can be computed numerically at the edges of the cells. This first step is written as:

$$\mathbf{U}_i^* = \mathbf{U}_i^n - \frac{\Delta t}{A_i} \left(\sum_{k=1}^3 (\mathbf{E}^* + \mathbf{H})_{i,k}^n \mathbf{n}_{i,k} l_k \right) \quad ; \quad \mathbf{H} = \begin{bmatrix} 0 & 0 \\ \frac{1}{2}gh|_{\eta_o}^2 & 0 \\ 0 & \frac{1}{2}gh|_{\eta_o}^2 \end{bmatrix} \quad (3)$$

where A_i is the area of cell Ω_i , Δt is the time step, the superscript n represents the time level, subindex k is used to denote the k -th edge of a cell, l_k is the length of edge k , $\mathbf{E}^* = (\mathbf{F}^*, \mathbf{G}^*)$ represents the numerical approximation

to \mathbf{E} , and $h|_{\eta_o}$ is the depth considering a piecewise constant free-surface elevation (*Valiani and Begnudelli, 2006*). The numerical fluxes \mathbf{F}^* and \mathbf{G}^* are computed using the central-upwind method of *Kurganov and Petrova (2005)*. In the second step the friction term is accounted to update the solution to time level $n + 1$ from the values of \mathbf{U}_i^* . Friction slope components S_{fx} and S_{fy} are computed using Manning's equation

$$S_{fx} = \frac{n^2 u \|\mathbf{u}\|}{h^{4/3}} \quad S_{fy} = \frac{n^2 v \|\mathbf{u}\|}{h^{4/3}} \quad (4)$$

185 where n is the Manning's coefficient and $\|\mathbf{u}\|$ is the l^2 -norm of the velocity
 186 vector \mathbf{u} . It is widely recognised that at very shallow depths, an explicit
 187 discretisation of the friction terms can cause an overshooting of friction that
 188 often leads to source term instability. In order to avoid this problem, time
 189 integration of the friction term is performed using an implicit scheme widely
 190 adopted by other shallow-water models (e.g. *Yoon and Kang, 2004; Sanders,*
 191 *2008; Liang and Marche, 2009; de Almeida et al, 2012*):

$$(hu)_i^{n+1} = \frac{(hu)_i^*}{1 + \Delta t g [n^2 \|\mathbf{u}\| / (h)^{4/3}]_i^n} \quad (5)$$

$$(hv)_i^{n+1} = \frac{(hv)_i^*}{1 + \Delta t g [n^2 \|\mathbf{u}\| / (h)^{4/3}]_i^n} \quad (6)$$

192 Free-surface reconstruction and wetting and drying are handled by the
 193 volume/free-surface method (VFR) of *Begnudelli and Sanders (2006)*, which
 194 provides a second-order accurate representation of the bed topography (*Begnudelli and Sanders, 2006; Begnudelli et al., 2008*). This further enhances
 195 the accuracy in the description of the terrain given by the extremely fine-
 196 resolution topography used in this paper. The stability of the model is controlled by the standard Courant-Friedrichs-Lewy (CFL) condition.

199 The model includes only the surface component of urban drainage. This
 200 allows us to separate the influence of the urban terrain on the flood inundation from the rather complex interactions that can take place between
 201 surface and the sewerage flows. While a realistic representation of real world
 202 inundation requires the dynamic coupling of the two processes (*Mark et al, 2004; Aronica and Lanza, 2005; Nasello and Tucciarelli, 2005; Maksimovic et al, 2009; Bazin et al, 2014*), the study of the surface component alone is
 203 appropriate for the objectives of the present analysis.
 204
 205
 206

207 3. Test cases

208 A set of four test cases are presented in this section to analyse the influ-
 209 ence of small scale changes in urban topography on the dynamics and final
 210 distribution of flooding. The tests use a 10 cm resolution digital elevation
 211 model produced from terrestrial LiDAR data collected by the Environment
 212 Agency of England and Wales (*Ozdemir et al*, 2013) in the urban area of Al-
 213 cester (Warwickshire, UK), which is shown in Figure 2.a. The computational
 214 mesh generated using this DEM is composed of 3, 575, 123 nodes, 10, 711, 014
 215 edges and 7, 135, 888 triangular elements. Figure 3 shows this computational
 216 mesh close to a street junction, illustrating how fine scale elements such as
 217 curbs are represented in the model. Such a fine resolution model captures
 218 the shape of road cambers extremely accurately (as shown by *Ozdemir et*
 219 *al*, 2013), and the use of a second order model for the bed slope terms (in
 220 which the terrain is represented as inclined, rather than horizontal triangles,
 221 as described in *Begnudelli and Sanders*, 2006 and *Begnudelli et al.*, 2008)
 222 brings the level of model representation of topography to a unprecedented
 223 level.

224 Small scale modifications have been introduced to the original topogra-
 225 phy in the two regions of the domain indicated with ellipses in Figure 2.a.
 226 These modifications have been strategically defined from the observation of
 227 the simulations using the undisturbed topography. Namely, the combined
 228 inspection of the road topography, topology and the characteristics of the
 229 flood propagation indicated potential regions of the domain where the effect
 230 of topographical manipulations could lead to significant changes in the evo-
 231 lution and final distribution of flooded areas. The extent and magnitude of
 232 these alterations can be observed by comparing Figures 2.b and 2.d against
 233 Figures 2.c and 2.e, respectively. In the first of these modifications, the ele-
 234 vation of the road in Figure 2.b is reduced over a distance of approximately
 235 30 m and by a maximum value of 18 cm (Figure 2.c). The second alteration
 236 was the introduction of a short hump (placed perpendicularly to the road
 237 direction and spanning from curb to curb) that increases the road elevation
 238 by a maximum value of 12 cm (from Figure 2.d to 2.e). Finally, a third
 239 scenario was generated by combining these two modifications into one DEM.
 240 Along with the original DEM, this provides four different scenarios that can
 241 be compared to analyse the influence of decimetric scale changes of the to-
 242 pography on inundation dynamics. All scenarios use exactly the same mesh
 243 topology, and only differ in the elevation of the road in the specific areas of

the domain described above.

The flow boundary condition used in the simulations follows that previously adopted and described by *Ozdemir et al* (2013), which was derived by assuming a 200-year return period 30-min rainfall that is collected over a drainage area upstream of the inflow point. The discharge increases linearly from $0 \text{ m}^3\text{s}^{-1}$ to the peak value ($0.35 \text{ m}^3\text{s}^{-1}$) during the first 7.5 min, is kept constant for the subsequent 15 min, after which it falls linearly to $0 \text{ m}^3\text{s}^{-1}$ during the final 7.5 min (Figure 4). This boundary condition is uniformly distributed across the road situated on the North-East end of the computational domain in Figure 2.a. All other boundary edges were set as solid walls. While this last choice misrepresents the dynamics of the flood propagation close to the boundaries, it has the advantage of keeping all the inflow within the domain, which is convenient to visualise how the water is distributed across the urban area at different stages of the flood wave propagation. The value of Manning’s coefficient was set to $n = 0.013$ for roads and pavements, and $n = 0.035$ elsewhere.

4. Results and discussion

Figure 5 shows the results of the four simulations at $t = 12, 30$ and 60 min. This figure illustrates the effects of the modifications introduced to the original topography on the flood dynamics. In all simulations the flood wave initially propagates southward along the main road located on the East side of the domain. As the water reaches street junctions, part of the flow can be diverted to side streets, depending on the local topography of the junction and neighbouring streets. For example, in Figure 5.a, the water passes by the first junction without being diverted. However, Figure 5.b shows that the reprofiling of the side street (presented in Figure 2.c) allows the water to flow along North-West direction, inundating a region of the domain that is dry during the simulation performed with the original topography (Figure 5.a). The volume of water diverted towards the North-West side of the domain in Figure 5.a is 69.8 m^3 , which represents approximately 15% of the total flow input into the domain during the simulation. The marked difference observed in this comparison was the result of an elevation difference of only 18 cm (maximum difference) between the two topographies.

The comparison of Figures 5.a and 5.c shows the influence of the 12 cm hump introduced to the original DEM (Figure 2.e). This small hump considerably reduces the amount of water that is diverted towards the street

280 where it was placed. Figure 6 shows further details of the flow close to
 281 the hump, illustrating how it almost completely prevents the water from
 282 flowing towards the side street. In addition, the partial blockage of this
 283 street diversion leads to more water being routed along the main road, which
 284 eventually accumulates in the Southern parts of the domain (as observed in
 285 the South-West part of the domain at $t = 60$ min, by comparing Figures 5.a
 286 and 5.c). Similarly, the diversion of part of the flood water towards the North-
 287 West part of the domain shown in Figure 5.b results in a decrease in the flow
 288 that is routed along the main road towards the South of the domain. The
 289 combined effects of these two modifications of the topography on the flooded
 290 areas is evidenced in Figure 5.d, which shows a considerable reduction in the
 291 volume of water that accumulates in the central part of the domain compared
 292 to the corresponding results in Figure 5.a. From $t = 0$ to $t = 60$ min, the
 293 total volumes of water diverted towards this side street in the central part
 294 of the domain are 231.8, 192.8, 14.2 and 5.1 m^3 in Figures 5.a, 5.b, 5.c and
 295 5.d, respectively. In other words, two targeted minor alterations of the urban
 296 topography were able to almost completely prevent the inundation of a part
 297 of the domain that would otherwise receive a significant proportion of the
 298 flood flow.

299 The results of the four simulations also show that the fine scale model
 300 often captures the type of flow that occurs at low depths, when the water
 301 flows exclusively close to the curbs (e.g. gutters), and does not inundate the
 302 crown of the road camber.

303 The results presented above show that model predictions of surface water
 304 flood in urban areas are highly sensitive to decimetric-scale features of the
 305 urban topography. In particular, the road topography close to junctions
 306 dictate whether diversions will occur, and therefore plays a crucial role in
 307 the aftermath of the urban floods. It has been observed that a minor (i.e.
 308 18 cm) and localized reduction of the road elevation can lead to significant
 309 inundation of areas that would otherwise not flood, while a small increase
 310 in the elevation (i.e. 12 cm) can prevent flood inundation from impacting
 311 relatively large parts of the urban domain.

312 The sensitivity of flood inundation to decimetric scale topography poses
 313 significant challenges for accurate assessments of flood risk in urban areas.
 314 First, it confirms the importance of high-resolution topographical datasets
 315 on the quality of model predictions, as previously indicated by *Ozdemir et*
 316 *al* (2013). This puts particular pressure on computational resources and
 317 methods. Secondly, it also raises questions on the accuracy that is needed for

the vertical position of topography datasets. Currently, terrain elevation data derived from airborne LiDAR that is usually used in flood risk assessment has a vertical accuracy of approximately 5 to 15 cm. While our results show that systematic elevation errors of this magnitude can have a significant impact on predictions of flood risk, it is unclear how randomly distributed measurement errors may affect the results.

The complexity of the inundation processes observed in the simulations, combined with the sensitivity of the results to small changes, also reaffirms standing questions on the limitations of simplified approaches adopted to modeling urban flooding. For instance, at shallow depths water typically flows exclusively along gutters, which operate as two separate and independent channels. With increasing depths, the flow eventually overtops the crown of the road camber and the two separate channels merge into a single cross section. This dynamics cannot be captured by 1D models, nor can it be reproduced by currently available sub-grid approaches.

While, on the one hand, the issues discussed above pose serious challenges for accurate modeling of floods in urban areas, they also unveil new opportunities for flood risk management. Namely, it has been shown that the final distribution of flood hazards can be significantly manipulated by introducing very small and localized changes to the topography of the road network. This could be used to divert flood waters away from critical parts of the urban area towards zones where the expected damage is limited or non-existent (e.g. parks or green areas). The possibility of using the road network as efficient open-channels to transport excess flood waters across the domain could provide a new set of engineering techniques to expand current methods used in urban drainage (which are largely limited to the function of delivering water to the sewer system). Such approach would fill an existing gap in flood risk management, which lacks cost-effective measures to mitigate the impacts of medium to extreme storm events. While high-frequency, low magnitude events can usually be tackled by a combination of traditional (e.g. sewer system design) methods and SuDS (e.g. soakaways, green roofs, pervious surfaces, etc), these will often have only a minor effect on large flooding disasters, and expanding these systems to accommodate larger events is unlikely to be cost-effective. Our results show that only minor changes in the urban topography are needed to drive significant changes to the impacts, which suggests that low cost risk mitigation could be achieved under this proposed framework.

355 5. Summary and conclusions

356 This article analyzes the influence of small changes in the topography
357 of the urban terrain on the propagation and final distribution of flooding
358 in urban areas. Numerical simulations have been performed using a highly
359 accurate finite volume shallow water model and an extremely fine resolution
360 (i.e. 10 cm) topography of a real urban area in the United Kingdom. This
361 provided an unprecedented level of detail in the representation of the dy-
362 namics of flood inundation over the urban terrain. Four different test cases
363 were produced by introducing minor (decimetric scale) modifications to the
364 original urban topography.

365 The results of these numerical experiments have shown that small alter-
366 ations in the urban topography can lead to contrastingly different patterns
367 of flood inundation. Namely, the combination of two targeted and minor
368 modifications – whereby the elevation of the road has been locally lowered
369 by 18cm and raised by 12cm – has almost completely prevented flooding
370 from impacting a large proportion of the modelled domain.

371 The sensitivity of flood inundation to small changes in the urban topog-
372 raphy gives rise to a number of challenges. First, capturing the effect of
373 small scale features requires finely resolved data that is rarely available for
374 the great majority of model simulations that are currently performed for
375 practical engineering studies. Second, not only the resolution of the datasets
376 is important, but the accuracy of the vertical position also becomes a issue
377 of high relevance. Airborne LiDAR datasets currently available have a ver-
378 tical accuracy of approximately 5 to 15 cm, which is of the same order of
379 magnitude of typical depths that occur when the overland flood flow is con-
380 veyed by road networks. Finally, the computational cost of modelling flood
381 inundation at these scales is in general too high, or even unfeasible for most
382 practical applications. This is particularly true when multiple simulations
383 are required, which is typically the case in probabilistic risk assessments and
384 engineering assessment of multiple scenarios.

385 While the dependency of flood inundation on small scale topography dis-
386 cussed above poses a number of practical difficulties to accurate assessments
387 of flood risk, it also paves the way to new possibilities of risk mitigation
388 that have not been explored to date. Namely, significant changes in the final
389 distribution of flood hazards could be achieved by manipulating the topog-
390 raphy at key regions of the urban domain. This could be used to divert part
391 of the flood flow away from critical parts of the urban areas, or to guide the

392 flood wave towards low impact zones (e.g. parks). As our results illustrate,
393 only minor and localized modifications in the topography may be needed
394 to produce substantial change to flood hazards, indicating that considerable
395 mitigation can be achieved at low cost. The simulation results presented
396 in this article also suggest that alterations in the road topography nearby
397 road junctions can be particularly effective in producing major changes in
398 the dynamics of flood propagation. This is because in these areas the local
399 topography dictates how much water is diverted towards different parts of
400 the urban domain, and therefore plays a crucial role in the aftermath of the
401 urban flood.

402 The challenges and opportunities highlighted in this article are inher-
403 ently interrelated. The level of detail needed for the design and optimiza-
404 tion of the surface drainage methods proposed above can only be achieved
405 in practice by enhanced availability of high-quality topographical data and
406 high-performance computational resources and techniques.

407 Finally real-world urban flood inundation can be influenced by a number
408 of issues that are not taken into account in our numerical analysis, including
409 interactions with the sewer system. While the results presented in this ar-
410 ticle provide strong evidences of the influence of small scale topography on
411 the surface component of inundation, further research is needed to under-
412 stand potentially important interactions between these mechanisms and the
413 sewerage system.

414 6. Acknowledgements and data access information

415 The Environment Agency of England and Wales (EA) is acknowledged for
416 providing the terrestrial LiDAR data used in this article. This data is copy-
417 righted and can be requested under licence from the EA ([www.environment-](http://www.environment-agency.gov.uk)
418 [agency.gov.uk](http://www.environment-agency.gov.uk)). All model results will be made available under request to
419 the corresponding author.

420 7. References

- 421 Aronica, G. T. and L. G. Lanza (2005), Drainage efficiency in urban areas: a
422 case study, *Hydrological Processes*, 19 1105–1119, DOI: 10.1002/hyp.5648
- 423 Bates, P. D., M. S. Horritt, and T. J. Fewtrell (2010), A sim-
424 ple inertial for- mulation of the shallow water equations for efficient

425 two-dimensional flood inundation modelling,, *J. Hydrol*, 387 33-45,
426 doi:10.1016/ j.jhydrol.2010.03.027.

427 Bazin, P-H, Nakagawa, H., Kawaike, K., Paquier, A. and E. Mignot (2014),
428 Modeling Flow Exchanges between a Streets and an Underground Drainage
429 Pipe during Urban Floods, *Journal of Hydraulic Engineering*, 140 No. 10,
430 04014051

431 Begnudelli, L. and B. Sanders (2006), Unstructured Grid Finite-Volume Al-
432 gorithm for Shallow-Water Flow and Scalar Transport with Wetting and
433 Drying, *Journal of Hydraulic Engineering*, 132 No. 4, 371–384

434 Begnudelli, L., Sanders, B. F., and S. F. Bradford (2008), Adaptive Godunov-
435 Based Model for Flood Simulation, *Journal of Hydraulic Engineering*, 134
436 No. 6, 714–725

437 Cunge J.A., Holly F.M. and A.Verwey (1980), Practical Aspects of Compu-
438 tational River Hydraulics. Pitman, London, U.K.

439 de Almeida, G. A. M., Bates, P. D., Freer, J., Souvignat, M. (2012), Im-
440 proving the stability of a simple formulation of the shallow water equa-
441 tions for 2D flood modelling. *Water Resources Research*, VOL. 48 ,
442 doi:10.1029/2011WR011570

443 de Almeida, G. A. M. and P. D. Bates (2013), Applicability of the local
444 inertial approximation of the shallow water equations to flood modeling
445 *Water Resources Research*, VOL. 49 , 1?12, doi:10.1002/wrcr.20366

446 DEFRA, 2008. Future Water: The Government?s Water Strategy for Eng-
447 land. CM7319 London.

448 Delleur, J. W. (2003), The Evolution of Urban Hydrology *Journal of Hy-*
449 *draulic Engineering*, 129, 563–573

450 Djordjevic S. Prodanovic D. and Maksimovic (1999), An approach to simu-
451 lation of dual drainage. *Water Science and Technology*, 39(9) 95-103

452 Dottori, F., Di Baldassarre, G. and E. Todini (2013), Detailed data is wel-
453 come, but with a pinch of salt: Accuracy, precision, and uncertainty in
454 flood modeling. *Water Resources Research*, 49 6079-6085

- 455 Environment Agency, 2009. Flooding in England: A National Assessment of
456 Flood Risk, Environment Agency, Bristol, UK.
- 457 Evans, E. P., Simm, J. D., thorne, C. R., Arnell, N. W., Ashley, R. M.,
458 Hess, T. M., Lane, S. N., Morries, J., Nicholls, R. J., Penning-Rowsell,
459 E. C., Reynard, N. S., Saul, A. J., Tapsell, S. M., Watkinson A. R. and
460 H. S. Whether (2008), An update of the Foresight Future Flooding 2004
461 qualitative risk analysis. *Cabinet Office*, London.
- 462 Fang, Xing and D. Su (2005), An integrated one-dimensional and two-
463 dimensional urban stormwater flood simulation model *Journal of the*
464 *American Water Resources Association*, 42(3), 713-724.
- 465 Gallegos, H. A., Schibert, J. E. and B. F. Sanders (2009), Two-dimensional,
466 high-resolution modeling of urban dam-break flooding: A case study of
467 Balwin Hills, California *Advances in Water Resources*, 32, 1323-1335.
- 468 Gallien, T. W., Schibert, J. E. and B. F. Sanders (2011), Predicting tidal
469 flooding of urbanised embayments: A modeling framework and data re-
470 quirements *Coastal Engineering*, 58, 567-577.
- 471 Guinot, V. (2012), Multiple porosity shallow water models for macroscopic
472 modelling of urban floods *Advances in Water Resources*, 37, 40-72.
- 473 Kurganov, A. and G. Petrova (2004), Central-Upwind Schemes on Triangular
474 Grids for Hyperbolic Systems of conservation Laws. *Numerical Methods for*
475 *Partial Differential Equations*, 21, pp. 536-552
- 476 Leandro, J. Chen, A., Djordjevic, S. and D. A. Savic (2009), Comparison of
477 1D/1D and 1D/2D Coupled (Sewer/Surface) Hydraulic Models for Urban
478 Flood Simulation. *Journal of Hydraulic Engineering*, 135, No. 6 pp. 495-
479 504
- 480 LeVeque, R. J. (2002), Finite Volume Methods for Hyperbolic Problems, 257
481 pp., *Cambridge Univ. Press*, Cambridge, Mass.
- 482 Liang, Q. and F. Marche (2009), Numerical resolution of well-balanced shal-
483 low water equations with complex source terms *Advances in Water Re-*
484 *sources*, 32, 873-884

- 485 Maksimovic, C., Prodanovic, D., Boonya-Aroonnet, S., Leitao, J. P., Djord-
486 jevic, S., and R. Allitt (2009), Overland flow and pathway analysis for
487 modelling of urban pluvial flooding *Journal of Hydraulic Research*, 47,
488 512-523
- 489 Mark, O., Weesakul, S., Apirumanekul, C., Boonya-Aroonnet, S. and S.
490 Djordjevic (2004), Potential and limitations of 1D modelling of urban
491 flooding *Journal of Hydrology*, 299, 284-299
- 492 Mignot, E., Paquier, A. and S. Haider (2006), Modeling floods in a dense
493 urban area using 2D shallow water equations *Journal of Hydrology*, 327,
494 186-199
- 495 Molinaro, P., Di Filippo, A., and F. Ferrari (1994), Modelling of flood wave
496 propagation over flat dry areas of complex topography in presence of differ-
497 ent infrastructures. In *Proceedings of Specialty Conference on "Modelling
498 of flood propagation over initially dry areas"*, Milan, 20-30 June; 209-225
- 499 Nasello, C. and T. Tucciarelli (2005), Dual Multilevel Urban Drainage Model
500 *Journal of Hydraulic Engineering*, 131, No. 9, 748-754
- 501 Ozdemir, H., Sampson, C. C., de Almeida, G. A. M., and P. D. Bates (2013),
502 Evaluating scale and roughness effects in urban flood modelling using ter-
503 restrial LiDAR data *Hydrol. Earth Syst. Sci.*, 17, 4015-4030
- 504 Sampson, C., Fewtrell, T. J., Duncan, A., Shaad, K., Horritt, M. S. and P.
505 D. Bates (2012), Use of terrestrial laser scanning data to drive decimetric
506 resolution urban inundation models, *Advances in Water Resources*, Vol.
507 41, 1-17
- 508 Sanders, B. (2008), Integration of a shallow water model with a local
509 time step, *Journal of Hydraulic Research*, Vol. 46, No. 4, 466-475,
510 doi:10.3826/jhr.2008.3243
- 511 Sanders, B., Schubert, J. E. and H. A. Gallegos (2008), Integral formula-
512 tion of shallow-water equations with anisotropic porosity for urban flood
513 modeling, *Journal of Hydrology*, 362, 19-38
- 514 Soares-Fraza, S, Lhomme, J., Guinot, V., and Y. Zech (2008), Two-
515 dimensional shallow-water model with porosity for urban flood modelling,
516 *Journal of Hydraulic Research*, Vol. 46, No. 1, 45-64

- 517 Valiani, A. and L. Begnudelli (2006), Divergence form for bed slope source
518 term in shallow water equations, *Journal of Hydraulic Engineering*, 132
519 No. 7, pp. 652-665
- 520 Yoon, T. H. and S-K. Kang. (2004), Finite Volume for Two-Dimensional
521 Shallow Water Flows on Unstructured Grids, *Journal of Hydraulic Engi-*
522 *neering*, 130 No. 7, 678-688

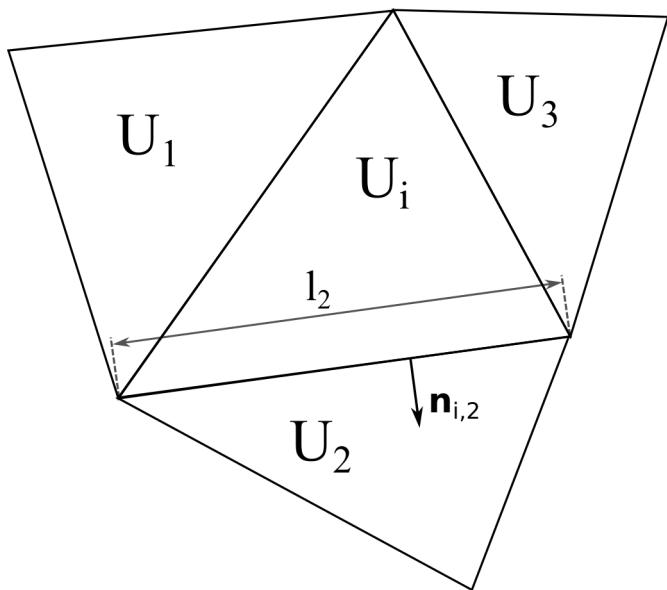


Figure 1: Ustructured computational mesh variables.

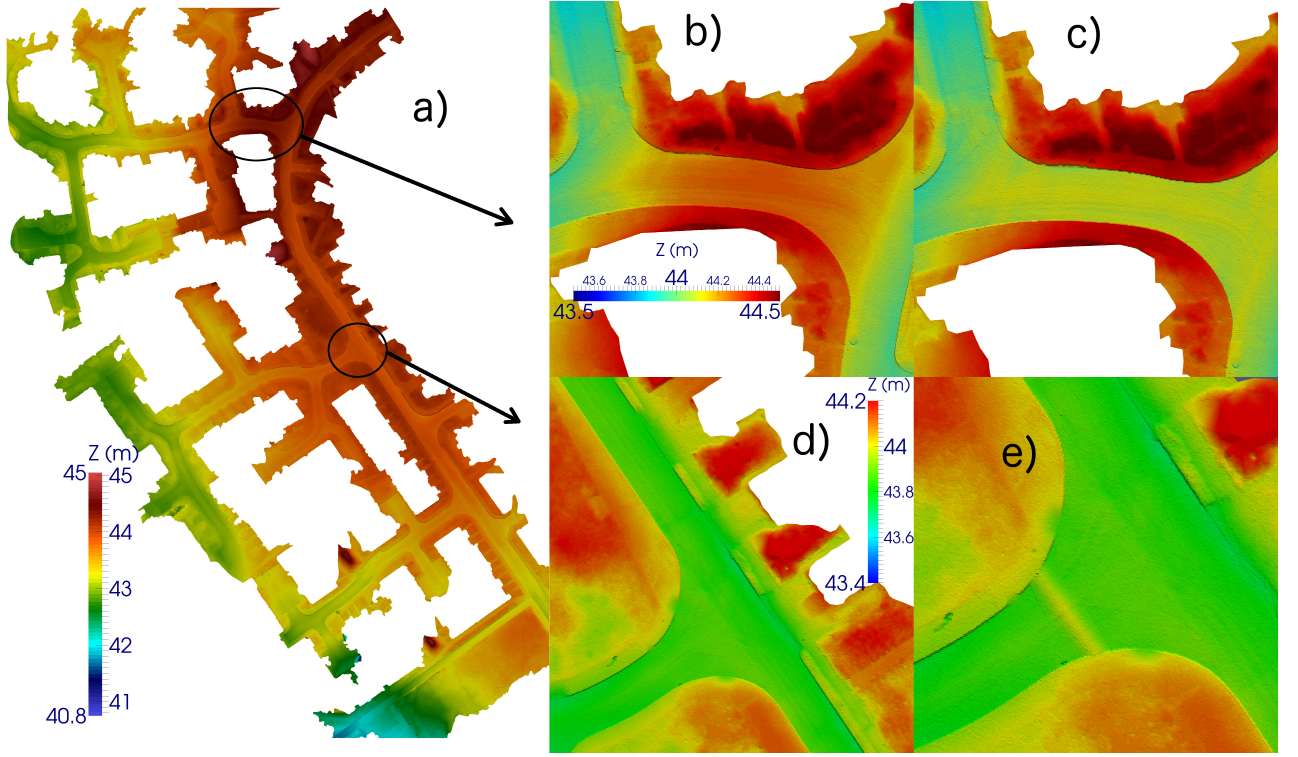


Figure 2: Original and modified DEMs. a) original DEM; b and d) zoom of the two regions indicated in the original DEM; c and e) modified DEMs.

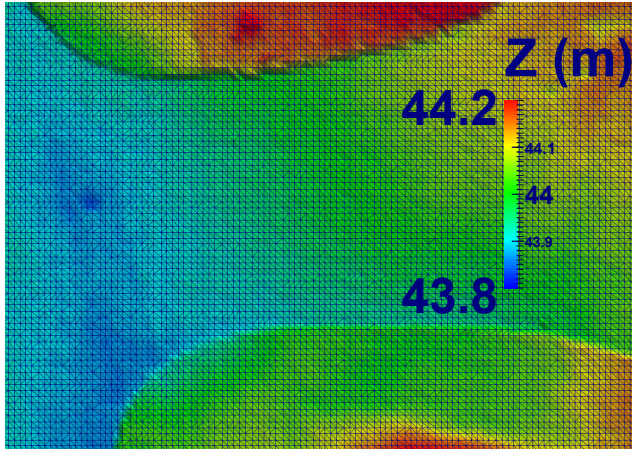


Figure 3: Detail of the computational mesh used.

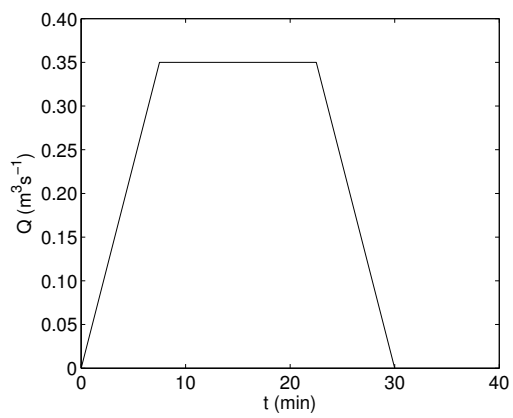


Figure 4: Hydrograph used as the upstream boundary condition.

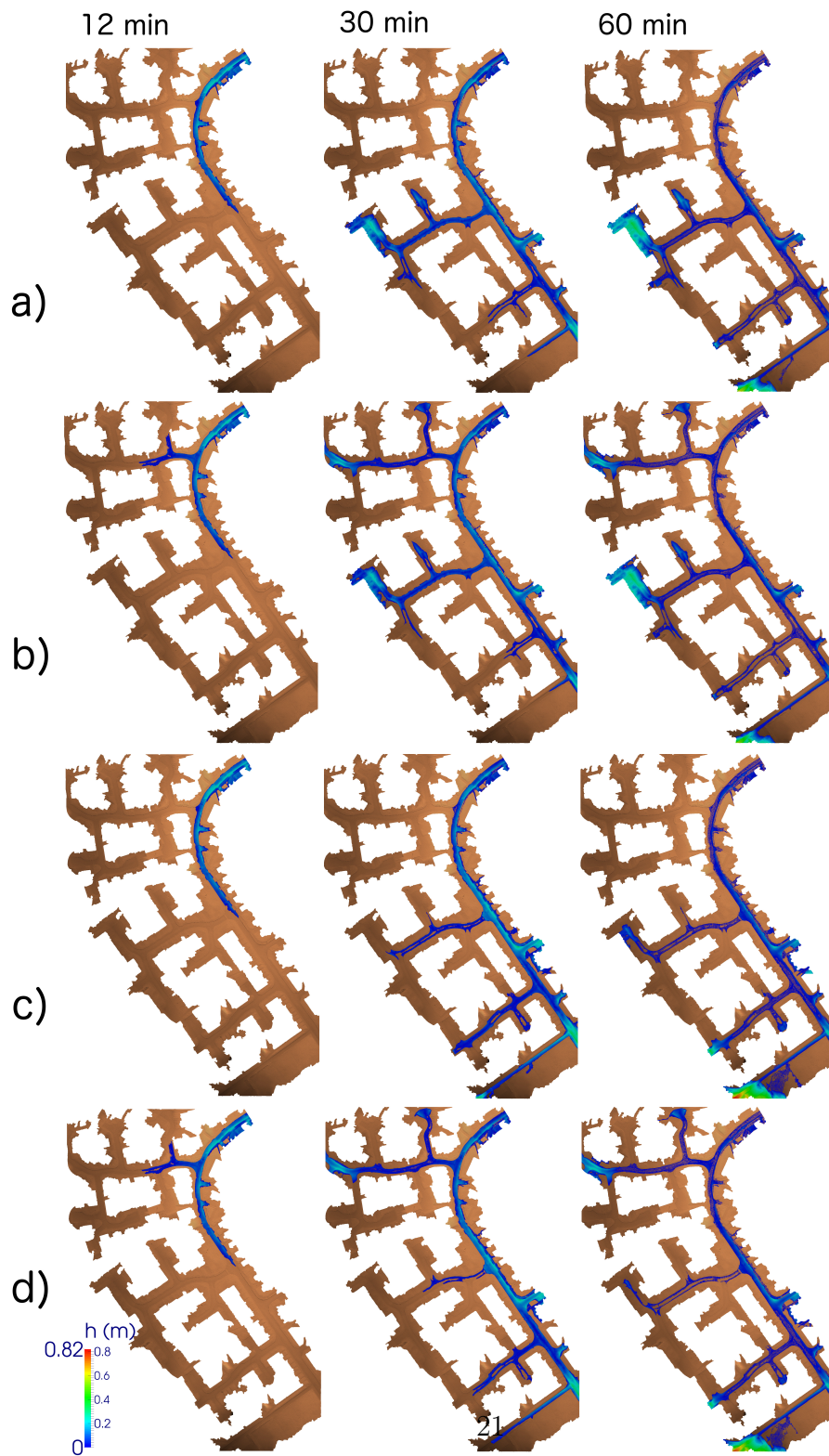


Figure 5: Results of the simulations at $t = 12, 30$ and 60 min and for the four scenarios. a) original topography; b) DEM modification corresponding Figure 1.c; c) DEM modification shown in Figure 1.e; d) combination of the two modifications.

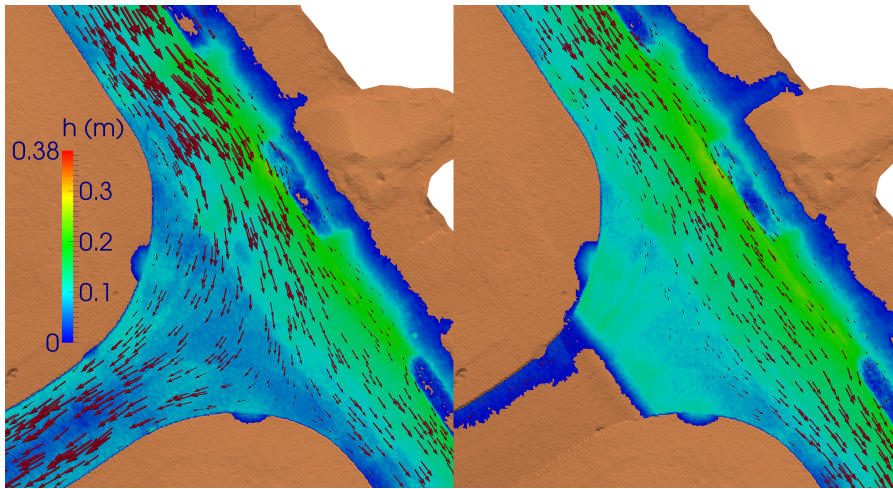


Figure 6: Detail of the flow close to the 12 cm hump at $t = 21$ min. Left: simulation with the original topography; Right: simulation with the hump introduced.